Original Article

Going from 3D/3D to 2D/3D registration for noncoplanar setup verification in intracranial single-isocenter multiple-target hypofractionated stereotactic radiotherapy: comparison between kilo-voltage/mega-voltage image pairs and noncoplanar cone-beam computed tomography

Jialu Lai[1]^, Shoupeng Liu[1], Jia Liu[2], Maoyue Fu[3], Maoqiong Jiang[3], An Li[1], Bin Li[1], Xinke Li[4], Xiaqin Cheng[5], Lin Zhou[5]

[1]Radiotherapy Physics & Technology Center, Cancer Center and State Key Laboratory of Biotherapy, West China Hospital, Sichuan University, Chengdu, China; [2]Department of Oncology, Chengdu First People's Hospital, Chengdu, China; [3]Department of Oncology, Yibin Second People's Hospital, Yibin, China; [4]West China Clinical Medical College of Sichuan University, Chengdu, China; [5]Thoracic Oncology Ward, Cancer Center and State Key Laboratory of Biotherapy, West China Hospital, Sichuan University, Chengdu, China

Contributions: (I) Conception and design: J Lai, S Liu, L Zhou; (II) Administrative support: L Zhou; (III) Provision of study materials or patients: J Liu, M Fu, M Jiang; (IV) Collection and assembly of data: A Li, B Li; (V) Data analysis and interpretation: J Lai, X Li, X Cheng, L Zhou; (VI) Manuscript writing: All authors; (VII) Final approval of manuscript: All authors.

Correspondence to: Lin Zhou, MD, PhD. Thoracic Oncology Ward, Cancer Center and State Key Laboratory of Biotherapy, West China Hospital, Sichuan University, No. 37 Guoxue Lane, Chengdu 610041, China. Email: zhoulin@wchscu.cn.

Background: Single-isocenter (SI) noncoplanar volumetric modulated arc therapy (NC-VMAT) has been widely used in stereotactic radiosurgery (SRS) or hypofractionated stereotactic radiotherapy (HSRT) for multiple brain metastases (BMs). However, it is critical to verify patient positioning at a noncoplanar couch angle. This study aimed to compare the noncoplanar setup discrepancies between kilo-voltage/mega-voltage image (kV/MV) orthogonal image pairs with a 2-dimensional/3-dimensional (2D/3D) matching mode and noncoplanar cone-beam computed tomography (NC-CBCT) with a 3D/3D matching mode in SI NC-VMAT HSRT for multiple BMs.

Methods: Twenty patients with multiple BMs [2–5] who underwent SI NC-VMAT HSRT were enrolled in this study. Prior to each noncoplanar field delivery, both kV/MV orthogonal image pairs and NC-CBCT were used to determine setup errors. The setup error values reported by NC-CBCT were defined as the gold standard and compared to those reported by kV/MV orthogonal image pairs. The Bland-Altman analysis method was utilized to assess the agreement of the two positioning modalities.

Results: In total, 104 kV/MV image pairs and NC-CBCT scans were acquired. The mean setup error differences (SEDs; absolute values) between the two positioning systems were 0.17 mm, 0.21 mm, 0.16 mm, 0.22°, 0.18°, and 0.17° in the vertical, longitudinal, lateral, yaw, pitch, and roll directions, respectively. The maximum SEDs regarding translation and rotation occurred in the longitudinal and yaw directions at 0.60 mm and 0.8°, respectively. Bland-Altman analysis showed excellent agreement between the two positioning modalities, and the 95% limits of agreement (LOAs) never exceeded 0.6 mm and 0.6° in the translational and rotational directions, respectively. Only 4.80% of SEDs exceeded the tolerance of 0.5 mm/0.5°.

Conclusions: Orthogonal kV/MV image pairs with 2D/3D matching mode could provide comparable

^ ORCID: 0000-0001-5940-1763.

accuracy for noncoplanar positioning as NC-CBCT with 3D/3D matching mode.

Keywords: Noncoplanar setup discrepancies; kilo-voltage/mega-voltage image orthogonal image pairs (kV/MV orthogonal image pairs); noncoplanar cone-beam computed tomography (noncoplanar CBCT); 2-dimensional/3-dimensional matching mode (2D/3D matching mode); 3-dimensional/3-dimensional matching mode (3D/3D matching mode)

Submitted Apr 08, 2023. Accepted for publication Sep 05, 2023. Published online Sep 28, 2023.
doi: 10.21037/qims-23-463
View this article at: https://dx.doi.org/10.21037/qims-23-463

Introduction

Current radiotherapy methods for multiple brain metastases (BMs) are shifting from whole brain radiation therapy (WBRT) to stereotactic radiosurgery (SRS) or hypofractionated stereotactic radiotherapy (HSRT) because of the better prognosis and fewer toxicity of SRS/HSRT compared to WBRT (1-4). Both SRS and HSRT require highly conformal and steep dose distributions to reduce the dose as low as possible to surrounding normal brain tissue (NBT) or critical organs at risk (OARs).

To achieve the above goals, a linear accelerator (LINAC)-based single-isocenter (SI) noncoplanar volumetric modulated arc therapy (NC-VMAT) delivery technique has been commonly employed (5-9). However, the successful application of such a technique is highly dependent on the patient positioning accuracy. One of the important issues is the setup uncertainty derived from couch rotation. Several studies have shown that setup errors occurred after the couch rotation, even though accurate patient positioning was achieved at a couch angle of 0° (10,11). These setup errors may degrade target coverage, result in increased damage to surrounding NBT and OARs, and thus adversely affect the treatment outcome. Utilizing a large planning target volume (PTV) margin may compromise the couch rotation-induced uncertainties to a certain degree, but it causes more NBT to be irradiated than necessary and increases the risk of radiation necrosis (12,13). Therefore, reverification of the patient setup after rotating the couch is particularly important for intracranial SI multiple-target NC-VMAT SRS/HSRT.

Cone-beam computed tomography (CBCT) has been widely used for patient positioning guidance during treatment (14,15). In our previous work, noncoplanar CBCT (NC-CBCT) was demonstrated to have excellent positioning accuracy for noncoplanar setup corrections based on a limited scanning range (150°–200°) and couch rotations (within ±45°). However, NC-CBCT has a relatively long image acquisition and setup verification time (approximately 2 min for each nonzero couch angle) (16), which will prolong the overall treatment time. Furthermore, for larger couch rotations (>±45°), using NC-CBCT for setup verification is nearly impossible due to the poor image quality caused by the small scanning range (<150°).

In addition to NC-CBCT, kilo-voltage/mega-voltage image (kV/MV) orthogonal image pairs with a 2-dimensional/3-dimensional (2D/3D) matching mode were demonstrated to have potential capability for noncoplanar setup verification (17-19). However, most previous works focused only on phantom measurements, which cannot fully mirror realistic clinical scenarios. kV/MV image pairs have several distinct advantages, including faster patient positioning verification at all possible couch angles with less ionizing radiation (20-22). To the best of our knowledge, no study has been conducted to compare the positioning accuracy of kV/MV image pairs to NC-CBCT at noncoplanar couch angles under treatment of intracranial multiple-target HSRT.

This study aimed to compare the setup discrepancies at nonzero couch angles measured by kV/MV orthogonal image pairs in 2D/3D matching mode and NC-CBCT in 3D/3D matching mode and determine whether kV/MV image pairs can be used as a noncoplanar image guidance method in SI NC-VMAT HSRT for multiple BMs.

Methods

Patient selection, contouring, and prescription

From May 2021 to October 2022, 20 patients with 2–5 BMs who received SI NC-VMAT HSRT were enrolled in the present study. This study was conducted in accordance with the Declaration of Helsinki (as revised in 2013). This study was reviewed and approved by the ethics committee

Table 1 Summary of patient, tumor, and treatment characteristics

Characteristics	Value
Age (years)	
Median	63
Range	42–80
Gender	
Male	9
Female	11
Site of the primitive tumor (n)	
NSCLC	16
Breast	4
No. of targets (n)	
2 lesions	5
3 lesions	8
4 lesions	4
5 lesions	3
No. of noncoplanar couch angles (n)	
For 2 lesions	1
For 3 lesions	2
For 4 lesions	2
For 5 lesions	2
PTV_{all} volume (cm^3)	
Median	11.7
Range	3.6–23.5
Dose/fractionation	
36 Gy/3	3
33 Gy/3	2
30 Gy/3	10
27 Gy/3	5

NSCLC, non-small cell lung cancer; PTV_{all}, composite planning tumor volumes for multiple-target patients.

of the West China Hospital and individual consent for this retrospective analysis was waived.

Each patient was positioned supine on the couch and immobilized using the frameless thermoplastic mask system (Sichuan Ruidi Medical Science and Technology Co., Ltd., Chengdu, China). All patients underwent computed tomography (CT) scans with 1-mm (n=13) or 2-mm (n=7) slice spacing, which were registered with magnetic resonance imaging (MRI) scans to define the gross tumor volume (GTV) and OARs. The GTV was uniformly expanded by a 2-mm margin to form the PTV. The PTVs of all metastases were combined into composite planning tumor volumes for multiple-target patients (PTV_{all}). In addition, the whole brain, optic pathway, lens, brain stem, eyes, cochlea, and basal ganglia were contoured as OARs. The prescription dose was 27–36 Gy in three fractions, which were based on the tumor size and location and was administered every other working day per fraction. All plans were normalized such that 99% of the PTV_{all} received a 100% prescribed dose. The median time interval between patient localization (CT/MRI) and radiotherapy was 5 days (range, 3–7 days). *Table 1* shows the patient, tumor, and treatment characteristics.

HSRT treatment planning and device

All HSRT plans were designed on a Varian Eclipse treatment planning system (TPS; v13.5, Varian Medical System, Palo Alto, USA) using the SI NC-VMAT delivery technique with 6 MV flattening filter free photon beams and a maximum dose rate of 1,400 monitor units per minute. All treatments were performed using Varian Edge™ LINAC (Varian, Palo Alto, California, USA), which was equipped with a high-definition multi-leaf collimator (MLC), a kV on-board imager (OBI) system, a MV electronic portal imaging device (EPID), and a PerfectPitch™ robotic couch for setup correction in six degrees of freedom (6DOF), including vertical, longitudinal, lateral, yaw, roll, and pitch directions (Figure S1). The OBI system includes a kV imaging panel mounted on the LINAC gantry orthogonally to the MV beam axis (Figure S1) and provides software for patient position verification, such as orthogonal kV/MV image pairs (2D/3D matching mode) and CBCT (3D/3D matching mode).

In this study, both coplanar and NC-CBCT images were acquired using OBI with a modified "head" scanning protocol (125 kV, 93.75 mAs) and a full-fan type, with a gantry speed of 6°/s. Axis slices were reconstructed using a field of view of 26.2 cm, 512×512 matrix, and 1.0-mm slice thickness, with a resolution of 0.51×0.51×1.00 mm^3. The kV images were obtained using 74 kV and 1.4 mAs. The MV images were obtained using the 2.5 MV imaging beam with a "High Quality" mode that typically required 1.5 monitor unit. For each plan, the treatment isocenter was positioned at the center of the PTV_{all}. In our previous work, NC-VMAT with limited couch rotation (within ±45°) combined

with NC-CBCT with a limited scanning range (150°–200°) was demonstrated to markedly improve the plan quality and setup accuracy in SI multiple-target HSRT (16). Therefore, the SI NC-VMAT plan contained a couch angle of 0° and one to two nonzero couch angles (*Table 1*), which were chosen from 30°, 330°, 45° and 315°. For each couch angle, 1–2 arcs were used, and the collimator angle of each arc was adjusted depending on the spatial distribution of the BMs so that optimal MLC movement could be achieved. To reduce out-of-field dose leakage, the jaw-tracking function was applied during planning optimization. In addition, to reduce the island blocking problem and in-field dose leakage, each plan was optimized using our previously proposed method, in which each arc only irradiates one or partial lesions (23,24). Dose calculation was performed using an analytical anisotropic algorithm (AAA) algorithm with 1-mm calculation grid.

Positioning system quality assurance

To avoid collisions, the available gantry rotation range for NC-CBCT scans and kV/MV image pair acquisition corresponding to different couch angles (Table S1) were determined via an anthropomorphic head phantom (Chengdu Dosimetric Phantom, Chengdu, China). An isoCal verification was run to verify the congruence of the kV and MV isocenters, which was found to be within 0.2 mm. At our institution, daily Winston-Lutz (W/L) tests demonstrated a mean isocentric accuracy of 0.30 mm. These shifts are within the tolerance of 1 mm recommended by the AAPM TG142 for SRS (25).

Patient setup procedure and treatment delivery

A flowchart showing the initial setup for treatment is given in *Figure 1*. The patient was initially aligned to the isocenter on the couch by matching room lasers to landmarks on the skin at a couch angle of 0°. Thereafter, the first coplanar CBCT image was acquired and registered to the reference planning CT created by the TPS system with the bony matching method. After automatic CBCT/planning CT registration or manual registration, when necessary, the calculated setup errors in 6DOF were corrected remotely from the console by using PerfectPitch^{TM} robotic couch. After that, a second CBCT scan was taken and again matched with planning CT to ensure that the shifts were applied correctly. If the residual setup error was within the specific tolerance of 0.5 mm/0.5°, the patient was considered accurately positioned. Otherwise, this correction process was repeated until the specific tolerance was eventually met, and then all arcs at a couch angle of 0° were treated. Then, the couch was rotated toward the nonzero angle, and the patient was imaged with orthogonal kV/MV image pairs, which were automatically registered with corresponding digitally reconstructed radiographs (DRRs) from planning CT using a user-defined region of interest including the whole skull and a 2D/3D matching mode. To ensure the accuracy of automatic image registrations, a senior therapist checked the overlap of the skull using the split view. If necessary, manual adjustments were made until the skull was completely aligned. Afterwards, the senior physician evaluated and reviewed the registration results. Finally, these reported shift values with kV/MV image pairs in 6DOF were recorded.

Without applying correction shifts from kV/MV image pairs to the couch, NC-CBCT was acquired and matched with reference planning CT using the 3D/3D matching mode. Then, calculated setup errors in 6DOF from NC-CBCT registrations were recorded for comparison with those from kV/MV orthogonal image pairs. Again, if the resulting setup errors reported by NC-CBCT exceeded the tolerance, the corresponding correction was applied with the aid of the PerfectPitch^{TM} robotic couch and verified by NC-CBCT until the setup error was within the tolerance and then the treatment was started. The whole setup procedure was repeated for every further couch rotation angle. Note that the patient position correction at the coplanar or noncoplanar couch angle was solely based on CBCT. To eliminate interobserver variability in the process, all registrations were performed by one experienced physician.

Statistical analysis

The percentage of absolute setup error differences (SEDs) (difference = kV/MV image pairs – NC-CBCT) between kV/MV image pairs and NC-CBCT >0.5 mm in translational directions or >0.5° in rotational directions was determined. The Bland-Altman method (26) was used to analyze the agreement between the two positioning systems. The 95% limits of agreement (LOAs) [mean ± 1.96 standard deviation (SD)] were determined to evaluate whether the difference between the upper and lower limits was within a clinically acceptable range (±0.5 mm and ±0.5°).

Results

In total, 104 pairs of kV/MV and NC-CBCT alignment

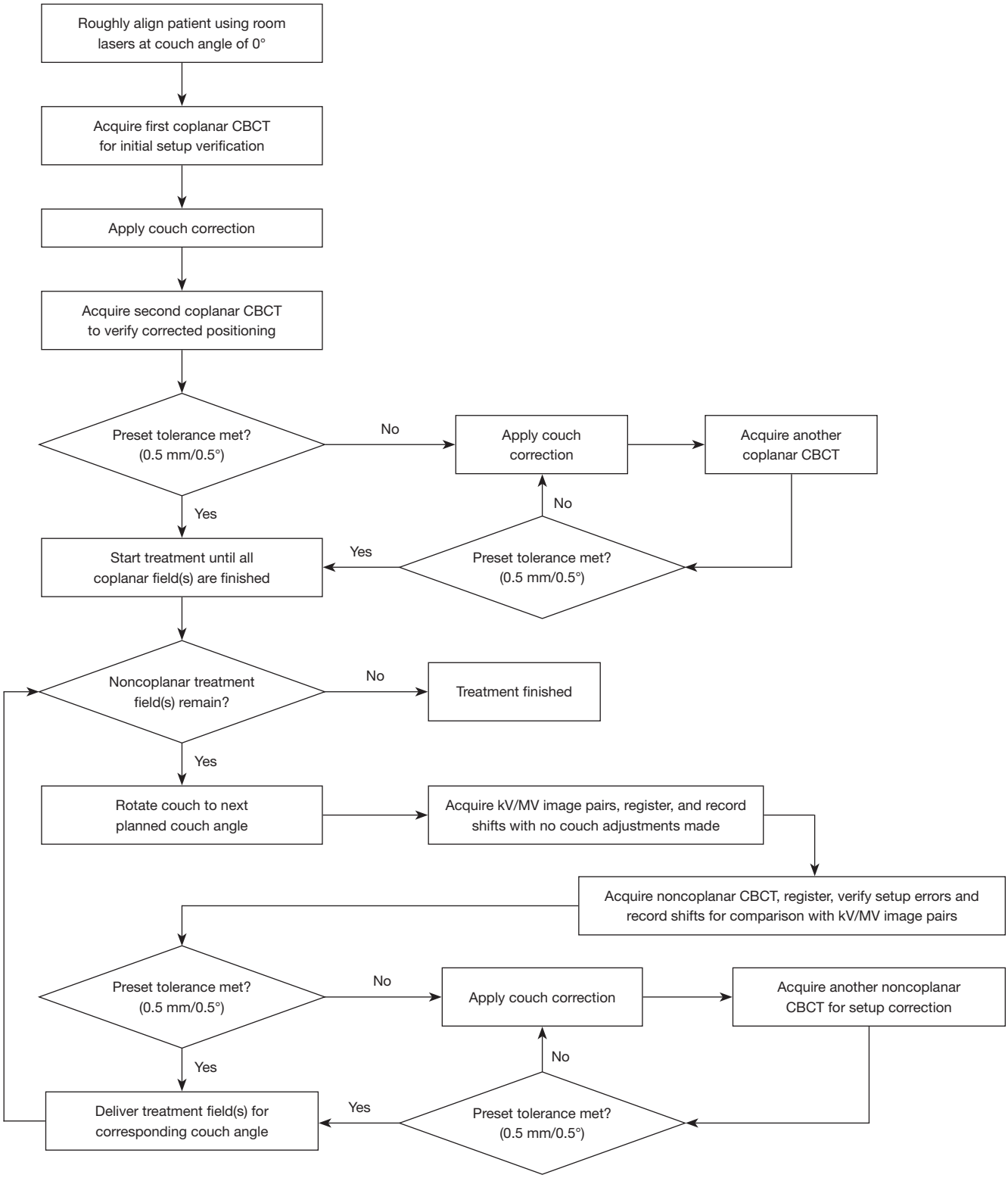

Figure 1 Flowchart of the workflow from patient positioning to treatment using CBCT and kV/MV image pairs in single-isocenter intracranial multiple-target hypofractionated stereotactic radiotherapy with noncoplanar volumetric modulated arc therapy. CBCT, cone-beam computed tomography; kV/MV, kilo-voltage/mega-voltage.

Table 2 Results of the absolute SEDs between kV/MV orthogonal image pairs and NC-CBCT for all patients, as well as the percentage of SEDs larger than 0.5 mm/0.5° between the readings via the two positioning methods in 6DOF

Difference	Translational (mm)			Rotational (°)		
	Vertical	Longitudinal	Lateral	Yaw	Pitch	Roll
Minimum	0.00	0.00	0.00	0.00	0.00	0.00
Maximum	0.50	0.60	0.40	0.80	0.60	0.50
Mean	0.17	0.21	0.16	0.22	0.18	0.17
Standard deviation	0.12	0.14	0.10	0.16	0.11	0.13
% of SEDs >0.5 mm or >0.5° in each direction (%)	0	0.96%	0	2.88%	1.92%	0
% of SEDs outside 0.5 mm/0.5°	4.80%					

SEDs, setup error differences; kV/MV, kilo-voltage/mega-voltage; NC-CBCT, noncoplanar cone-beam computed tomography; 6DOF, six degrees of freedom.

sets were obtained from 20 patients. One kV/MV image pairs were not performed because of technical failure. The deviation between the setup errors of the two positioning methods was evaluated separately for each direction.

Table 2 shows the absolute SEDs between the kV/MV image pairs and NC-CBCT. The setup errors from the latter were designed as reference values. The mean (SD) of the absolute SEDs was 0.17 (0.12) mm, 0.21 (0.14) mm, 0.16 (0.10) mm, 0.22° (0.16), 0.18° (0.11), and 0.17° (0.13) in the vertical, longitudinal, lateral, yaw, pitch, and roll directions, respectively. Among the results, the maximum absolute SEDs regarding translation and rotation were 0.6 mm and 0.8°, which occurred in the longitudinal and yaw directions, respectively. The percentages of fractions with absolute SEDs >0.5 mm or >0.5° were 0%, 0.96%, 0%, 2.88%, 1.92% and 0% for the vertical, longitudinal, lateral, yaw, pitch, and roll directions, respectively. The percentage of absolute SEDs outside the tolerance of 0.5 mm/0.5° was 4.8%.

Figure 2 shows the Bland-Altman plots (*Figure 2A*) and summarizes the distribution of the percent inverse cumulative frequency of absolute SEDs in 6DOF (*Figure 2B*). The mean deviation and 95% LOA of the two positioning modalities were –0.01 (–0.43 to 0.41) mm, 0.18 (–0.18 to 0.53) mm, 0.05 (–0.30 to 0.40) mm, 0.04° (–0.49 to 0.57°), –0.10° (–0.46 to 0.26°) and –0.00096° (–0.42 to 0.42°) for the vertical, longitudinal, lateral direction, yaw, pitch, and roll directions, respectively. *Figure 3* shows a representative example for image registrations at a couch angle of 315° using both positioning systems. The setup differences between the two positioning systems were found to be small in 6DOF (red wireframe).

Discussion

In this study, we evaluated the consistency of couch shifts reported by two positioning systems regarding noncoplanar setup verification, namely, kV/MV orthogonal image pairs with 2D/3D matching mode and NC-CBCT with 3D/3D matching mode. The results clearly showed that there were very small differences in shift values between the two positioning methods. To the best of our knowledge, this is the first report focusing on evaluating shift detection discrepancy between kV/MV orthogonal image pairs and NC-CBCT in HSRT for multiple intracranial BMs under clinical conditions.

Intracranial SI multiple-target HSRT places great demands on patient positioning accuracy due to the high dose per fraction, steep dose gradient, and heightened sensitivity to setup error, especially for small lesions and those far from the isocenter (27,28). Such characteristics leave little room for intracranial SI multiple-target HSRT to average out positional errors in the conventional multifractionated treatment course, and it is important to reverify the patient position after rotating the couch (29). In our previous study, we found that even setup correction was made at the 0° couch angle, but 57.10% of the measured noncoplanar setup errors still exceeded the tolerance of 0.5 mm/0.5° after rotating the couch for noncoplanar treatment in intracranial HSRT (16).

Currently, both kV/MV orthogonal image pairs and NC-CBCT are available for noncoplanar setup verification. Overall, the absolute SEDs between the two positioning systems was small at 6DOF, with maximum absolute SEDs of 0.6 mm and 0.8° in the translational and rotational directions (*Table 3*), respectively. Although the upper 95%

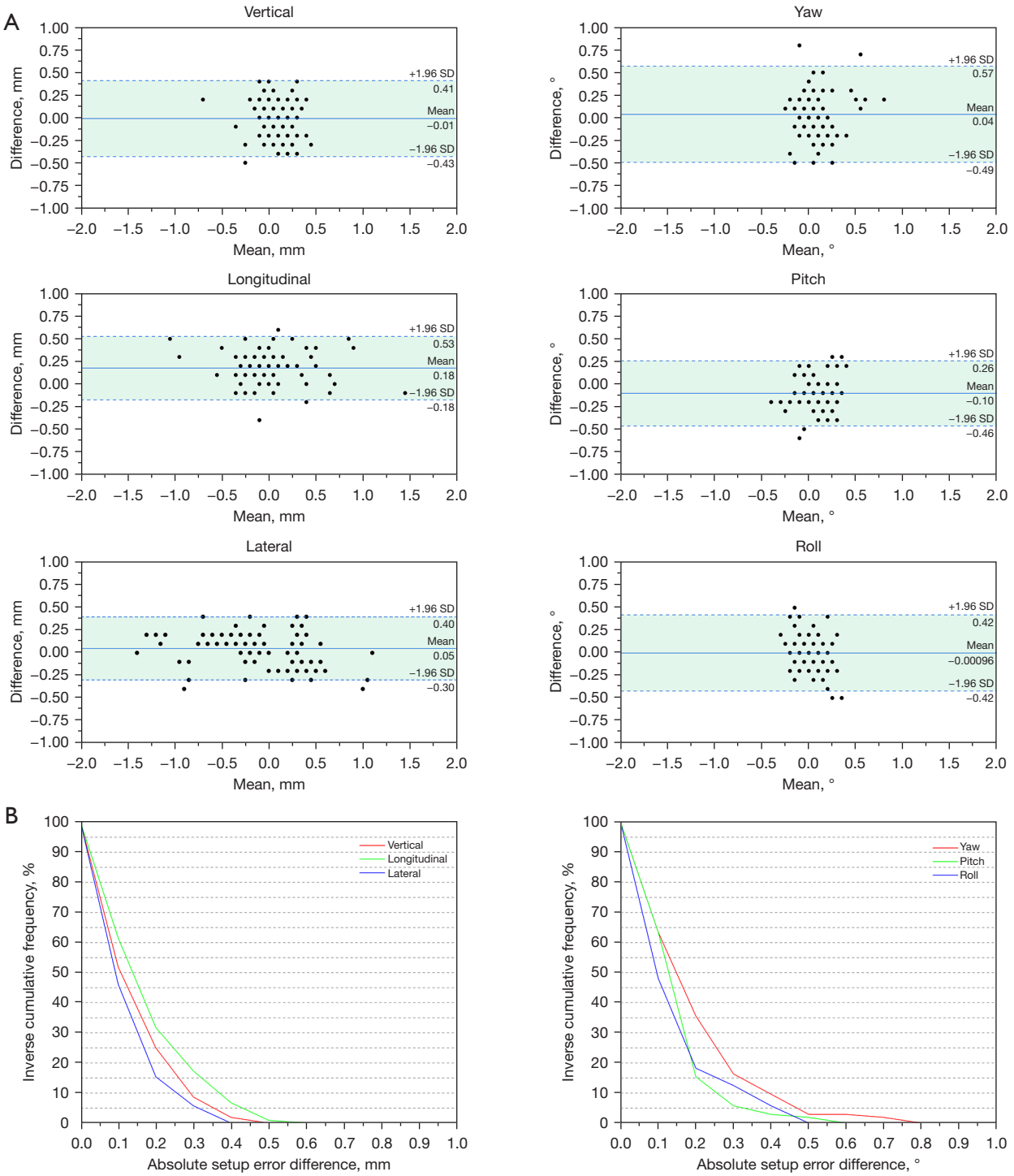

Figure 2 Evaluation results of the absolute SEDs between two matching modes. (A) Bland-Altman plots of the difference between kV/MV image pairs and NC-CBCT-based couch shifts; (B) distribution of inverse cumulative frequency of absolute SEDs between two positioning systems with respect to 6DOF. SD, standard deviation; SEDs, setup error differences; kV/MV, kilo-voltage/mega-voltage; NC-CBCT, noncoplanar cone-beam computed tomography; 6DOF, six degrees of freedom.

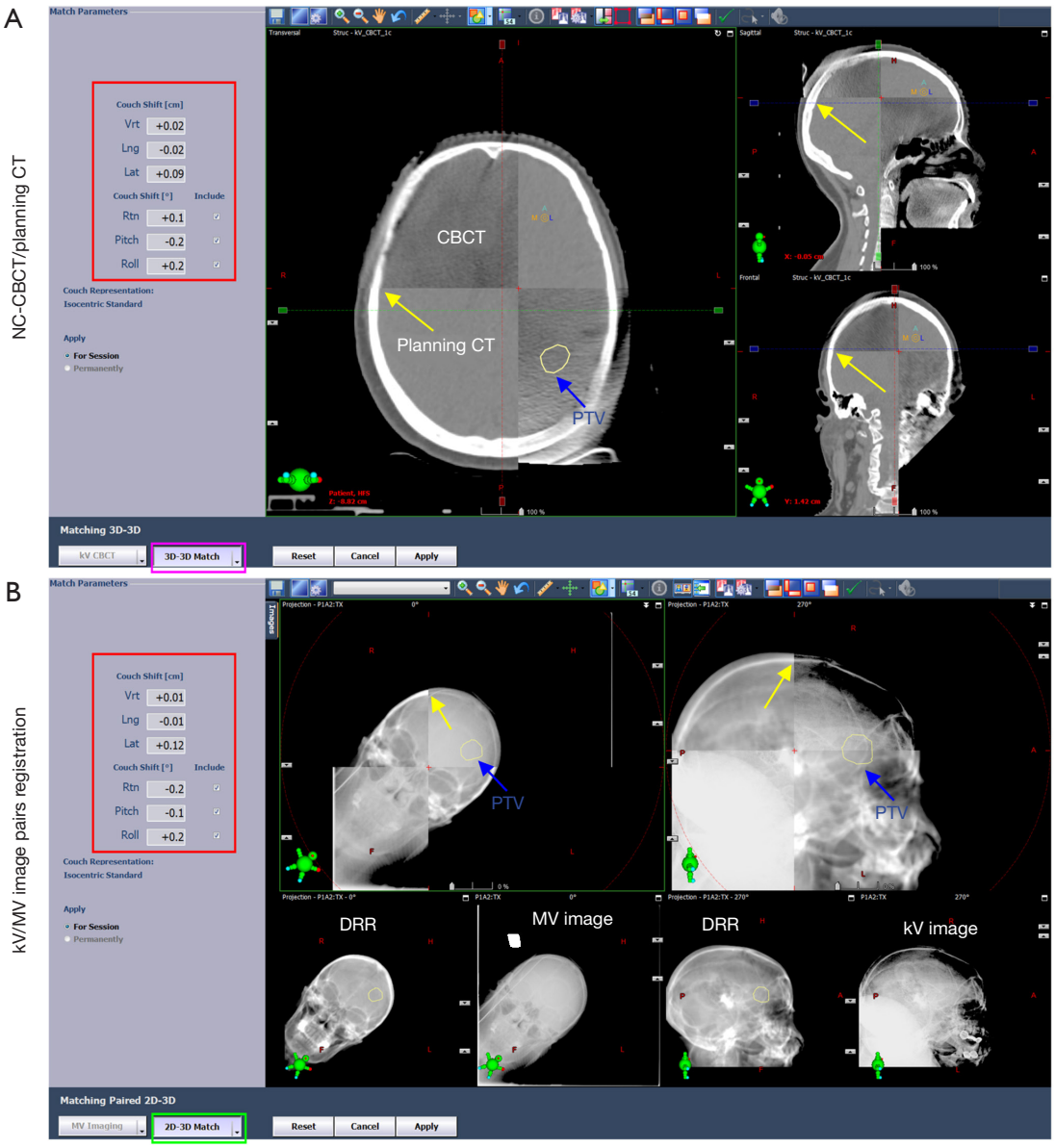

Figure 3 Registrations of actual positioning image with planned positioning image by both systems at a couch angle of 315°. (A) Registration between NC-CBCT and planning CT with 3D/3D matching mode (purple wireframe). (B) Registration between kV/MV orthogonal image pairs and corresponding DRR images with 2D/3D matching mode (green wireframe). The setup error was presented as the "couch shift" value after aligning the registration (red wireframe). Note that brain lesions were not visible on either NC-CBCT or kV/MV images. Therefore, both positioning systems were performed based on the bony anatomy of the skull (yellow arrows). NC-CBCT, noncoplanar cone-beam computed tomography; CT, computed tomography; PTV, planning target volume; R, right; L, left; A, anterior; P posterior; H, head; F, foot; HFS, head-first supine; kV/MV, kilo-voltage/mega-voltage; DRR, digitally reconstructed radiograph; 2D, 2-dimensional; 3D, 3-dimensional.

of LOA in the longitudinal direction (0.53 mm) and yaw direction (0.57°) exceeded the tolerance of 0.5 mm/0.5°, more than 95% of the absolute SEDs of the measurement pairs met the tolerance value (*Table 2*). It should, however, be noted that the accuracy of both positioning systems is limited by the resolution of couch digital readouts, which

Table 3 Results of the absolute SEDs between kV/MV orthogonal image pairs and NC-CBCT regarding different CT slice thicknesses (1-mm CT slice thickness for 13 patients; 2-mm CT slice thickness for 7 patients), as well as the percentage of SEDs larger than 0.5 mm/0.5° between the readings via the two positioning methods in 6DOF

Difference	With 1-mm CT slice thickness for noncoplanar setup verification (n=39)						With 2-mm CT slice thickness for noncoplanar setup verification (n=65)					
	Translational (mm)			Rotational (°)			Translational (mm)			Rotational (°)		
	Vertical	Longitudinal	Lateral	Yaw	Pitch	Roll	Vertical	Longitudinal	Lateral	Yaw	Pitch	Roll
Minimum	0	0	0	0	0	0	0	0	0	0	0	0
Maximum	0.50	0.50	0.40	0.70	0.60	0.50	0.40	0.60	0.40	0.80	0.50	0.50
Mean	0.18	0.17	0.15	0.22	0.18	0.16	0.17	0.28	0.17	0.22	0.17	0.18
Standard deviation	0.13	0.11	0.10	0.16	0.12	0.13	0.11	0.15	0.11	0.18	0.11	0.13
% of SEDs >0.5 mm or >0.5° in each direction	0	0	0	1.54%	3.08%	0	0	2.56%	0	5.13%	0	0

SEDs, setup error differences; kV/MV, kilo-voltage/mega-voltage; NC-CBCT, noncoplanar cone-beam CT; 6DOF, six degrees of freedom.

is 0.1 mm for translational directions and 0.1 degrees for rotational directions. This means that the tolerance of 0.5 mm/0.5° in the present study can be considered equivalent to the tolerance of <0.6 mm and <0.6°. Therefore, it can be concluded that excellent agreement between the two positioning methods was achieved in terms of noncoplanar setup verification, suggesting that kV/MV image pairs can be used accurately for setup verification at noncoplanar couch angles.

However, it is interesting to note that absolute SEDs in the longitudinal and yaw directions were larger than those in other translational and rotational directions, respectively. Li *et al.* (30) have also reported similar results by investigating the positioning discrepancies between Varian CBCT and oblique kV/kV image pairs from BrainLab ExacTrac X-ray (BrainLAB AG, Feldkirchen, Germany) for setup verification in intracranial radiosurgery. There are several potential reasons for this phenomenon. First, the difference in CT slice thickness might be a potential source of observed differences. The reference CT images in this study had two slice thicknesses, i.e., 1 and 2 mm. However, the CT image resolution in other directions (vertical and lateral) was the same for both kinds of CT, which was 0.97 mm. Therefore, image registration could introduce a larger uncertainty in the longitudinal direction. We analyzed the discrepancy of SEDs in 6DOF from NC-CBCT registrations and kV/MV orthogonal image pairs in different CT slice thicknesses, and larger SEDs in the longitudinal direction were observed for CT scans with 2 mm (n=7) slice spacing (*Table 3*). However, because of the limited number of patients in each group (13 patients *vs.* 7 patients), a statistical analysis of the difference between the two groups was not performed. Murphy *et al.* (31) have demonstrated that the precision of head positioning improves by a factor of 2 when the CT slice thickness is reduced from 3.0 to 1.5 mm. More measurements are necessary in the future to determine whether there is a permanent tendency for larger SEDs in the longitudinal direction.

Second, intrafraction patient motion might contribute to the found differences as well. Although the time interval between the kV/MV and NC-CBCT measurements was only a few minutes, patient motion might still occur between image acquisitions. Hoogeman *et al.* (32) conducted a study to quantify intrafractional patient motion and its time dependence in patients immobilized with thermoplastic masks and found that patients could still move, especially in the longitudinal and rotational directions. Third, the larger SEDs in the longitudinal direction might be due to systematic offsets inherent in kV and MV imaging systems, which induces higher systematic uncertainties in the longitudinal direction when using kV/MV image pairs or CBCT. Even using rigid registration for brain positioning, Chang *et al.* (33) found that the mean image registration accuracy of CBCT with conventional CT was 0.28 mm (SD =0.10). Therefore, high coincidence of kV imaging systems and MV beam delivery are essential for accurate image guidance. Further investigation on the reason why a larger SEDs between the two positioning systems occurred in the longitudinal and rotational directions is expected in

future studies. Another interesting observation is that the statistical data points exhibit a wider distribution along the x-axis direction in longitudinal and lateral directions than statistical data points in other directions (*Figure 2A*). This phenomenon can be explained by the fact that the relatively large setup errors are more likely to occur in the longitudinal and lateral directions after the couch rotation, which has been demonstrated by our previous study (16).

In some treatment sites, such as the lung, CBCT has obvious advantages over kV or MV portal imaging: it provides much more information about the tumor shape and location, where tumor-based positioning is available (34-36). However, one should note that most brain tumors, especially small tumors, could not be visualized clearly in both kV/MV portal images and NC-CBCT images (*Figure 3*), so both positioning systems use the skull-based matching method for setup verification, which has been demonstrated to be a reliable matching modality in intracranial HSRT (37). The successful registration of these two positioning systems is heavily dependent on the image quality, especially the visibility of the skull. In the present study, 2.5-MV portal imaging was used, which has advantages in terms of high- and low-contrast resolutions and contrast-to-noise ratio compared to 6-MV portal imaging (38). *Figure 3B* shows that both kV and MV images can identify the skull. However, the image quality of the 2.5-MV portal image was still slightly inferior to that of the kV portal image. In theory, kV/kV image pairs may achieve better setup verification, but it requires a gantry rotation between image acquisition. kV and MV imagers are naturally orthogonal to each other (Figure S1), which provide an easy implementation for noncoplanar setup verification because they reduce the time needed for gantry rotation and thus shorten the setup verification time. From the experience of our institution, the setup verification time with kV/MV image pairs for each noncoplanar couch angle is approximately 0.8 minutes, which is significantly less than the setup time of NC-CBCT (16).

Prentou *et al.* (39) investigated the dosimetric impact of setup errors on both targets and OARs and concluded that if OAR sparing was also a concern, for example, when OARs were very close to targets, more stringent tolerance values should be applied. In the present study, a tolerance of 0.5 mm/0.5° setup tolerance was applied, which was stricter than that reported by Gevaert *et al.* (40) (1 mm/0.5°) and Babic *et al.* (41) (1 mm/1°). The tighter tolerance value increases the dose delivery accuracy with the cost of increasing the number of positioning corrections, and using kV/MV image pairs instead of NC-CBCT may significantly shorten the overall setup verification time in SI NC-VMAT HSRT. More importantly, kV/MV image pairs can be used for setup verification even when larger couch rotations are introduced (>±45°), where using NC-CBCT for noncoplanar setup verification is not available.

There were some limitations in the present study. First, only a modest number of patients were enrolled. Additional studies with more patients and more images will be conducted in the future. Second, all patients were from the same hospital and thus possibly introduced some bias. Therefore, clinical investigations from more institutions are needed to validate the adequacy of these findings. Despite these limitations, the quantitative data of the present study regarding actual patients have some contribution to the active area in the study for noncoplanar setup verifications in SI NC-VMAT HSRT for multiple BMs.

Conclusions

kV/MV orthogonal image pairs with 2D/3D matching mode showed a good agreement with NC-CBCT with 3D/3D matching mode for noncoplanar setup correction in NC-VMAT HSRT for multiple BMs. Furthermore, kV/MV orthogonal image pairs require less time to assess patient setup with a lower radiation dose and therefore might be considered superior to CBCT in clinical practice.

Acknowledgments

Funding: This work was supported by the Sichuan Science and Technology Program (No. 2019YFS0323) and the National Natural Science Foundation of China (No. 81872466).

Footnote

Conflicts of Interest: All authors have completed the ICMJE uniform disclosure form (available at https://qims.amegroups.com/article/view/10.21037/qims-23-463/coif). The authors have no conflicts of interest to declare.

Ethical Statement: The authors are accountable for all aspects of the work in ensuring that questions related to the accuracy or integrity of any part of the work are appropriately investigated and resolved. This study was conducted in accordance with the Declaration of Helsinki (as revised in 2013). The study was approved by the ethics

committee of West China Hospital and individual consent for this retrospective analysis was waived.

References

1. Brown PD, Ballman KV, Cerhan JH, Anderson SK, Carrero XW, Whitton AC, Greenspoon J, Parney IF, Laack NNI, Ashman JB, Bahary JP, Hadjipanayis CG, Urbanic JJ, Barker FG 2nd, Farace E, Khuntia D, Giannini C, Buckner JC, Galanis E, Roberge D. Postoperative stereotactic radiosurgery compared with whole brain radiotherapy for resected metastatic brain disease (NCCTG N107C/CEC·3): a multicentre, randomised, controlled, phase 3 trial. Lancet Oncol 2017;18:1049-60.
2. Hartgerink D, Swinnen A, Roberge D, Nichol A, Zygmanski P, Yin FF, Deblois F, Hurkmans C, Ong CL, Bruynzeel A, Aizer A, Fiveash J, Kirckpatrick J, Guckenberger M, Andratschke N, de Ruysscher D, Popple R, Zindler J. LINAC based stereotactic radiosurgery for multiple brain metastases: guidance for clinical implementation. Acta Oncol 2019;58:1275-82.
3. Wegner RE, Leeman JE, Kabolizadeh P, Rwigema JC, Mintz AH, Burton SA, Heron DE. Fractionated stereotactic radiosurgery for large brain metastases. Am J Clin Oncol 2015;38:135-9.
4. Yamamoto M, Serizawa T, Higuchi Y, Sato Y, Kawagishi J, Yamanaka K, Shuto T, Akabane A, Jokura H, Yomo S, Nagano O, Aoyama H. A Multi-institutional Prospective Observational Study of Stereotactic Radiosurgery for Patients With Multiple Brain Metastases (JLGK0901 Study Update): Irradiation-related Complications and Long-term Maintenance of Mini-Mental State Examination Scores. Int J Radiat Oncol Biol Phys 2017;99:31-40.
5. Alongi F, Fiorentino A, Gregucci F, Corradini S, Giaj-Levra N, Romano L, Rigo M, Ricchetti F, Beltramello A, Lunardi G, Mazzola R, Ruggieri R. First experience and clinical results using a new non-coplanar mono-isocenter technique (HyperArc™) for Linac-based VMAT radiosurgery in brain metastases. J Cancer Res Clin Oncol 2019;145:193-200.
6. Clark GM, Popple RA, Young PE, Fiveash JB. Feasibility of single-isocenter volumetric modulated arc radiosurgery for treatment of multiple brain metastases. Int J Radiat Oncol Biol Phys 2010;76:296-302.
7. Ohira S, Ueda Y, Akino Y, Hashimoto M, Masaoka A, Hirata T, Miyazaki M, Koizumi M, Teshima T. HyperArc VMAT planning for single and multiple brain metastases stereotactic radiosurgery: a new treatment planning approach. Radiat Oncol 2018;13:13.
8. Parikh NR, Kundu P, Levin-Epstein R, Chang EM, Agazaryan N, Hegde JV, Steinberg ML, Tenn SE, Kaprealian TB. Time-Driven Activity-Based Costing Comparison of Stereotactic Radiosurgery to Multiple Brain Lesions Using Single-Isocenter Versus Multiple-Isocenter Technique. Int J Radiat Oncol Biol Phys 2020;108:999-1007.
9. Zhang S, Yang R, Shi C, Li J, Zhuang H, Tian S, Wang J. Noncoplanar VMAT for Brain Metastases: A Plan Quality and Delivery Efficiency Comparison With Coplanar VMAT, IMRT, and CyberKnife. Technol Cancer Res Treat 2019;18:1533033819871621.
10. Eder MM, Reiner M, Heinz C, Garny S, Freislederer P, Landry G, Niyazi M, Belka C, Riboldi M. Single-isocenter stereotactic radiosurgery for multiple brain metastases: Impact of patient misalignments on target coverage in non-coplanar treatments. Z Med Phys 2022;32:296-311.
11. Tanaka Y, Oita M, Inomata S, Fuse T, Akino Y, Shimomura K. Impact of patient positioning uncertainty in noncoplanar intracranial stereotactic radiotherapy. J Appl Clin Med Phys 2020;21:89-97.
12. Agazaryan N, Tenn S, Lee C, Steinberg M, Hegde J, Chin R, Pouratian N, Yang I, Kim W, Kaprealian T. Simultaneous radiosurgery for multiple brain metastases: technical overview of the UCLA experience. Radiat Oncol 2021;16:221.
13. Kirkpatrick JP, Wang Z, Sampson JH, McSherry F, Herndon JE 2nd, Allen KJ, Duffy E, Hoang JK, Chang Z, Yoo DS, Kelsey CR, Yin FF. Defining the optimal planning target volume in image-guided stereotactic radiosurgery of brain metastases: results of a randomized trial. Int J Radiat Oncol Biol Phys 2015;91:100-8.
14. Sun L, Jiang Z, Chang Y, Ren L. Building a patient-specific model using transfer learning for four-dimensional cone beam computed tomography augmentation. Quant Imaging Med Surg 2021;11:540-55.

15. Zhao W, Shen L, Islam MT, Qin W, Zhang Z, Liang X, Zhang G, Xu S, Li X. Artificial intelligence in image-guided radiotherapy: a review of treatment target localization. Quant Imaging Med Surg 2021;11:4881-94.
16. Lai JL, Liu SP, Liu J, Li XK, Chen J, Jia YM, Lei KJ, Zhou L. Clinical Feasibility of Using Single-isocentre Non-coplanar Volumetric Modulated Arc Therapy Combined with Non-coplanar Cone Beam Computed Tomography in Hypofractionated Stereotactic Radiotherapy for Five or Fewer Multiple Intracranial Metastases. Clin Oncol (R Coll Radiol) 2023;35:408-16.
17. Mancosu P, Fogliata A, Stravato A, Tomatis S, Cozzi L, Scorsetti M. Accuracy evaluation of the optical surface monitoring system on EDGE linear accelerator in a phantom study. Med Dosim 2016;41:173-9.
18. Oliver JA, Kelly P, Meeks SL, Willoughby TR, Shah AP. Orthogonal image pairs coupled with OSMS for noncoplanar beam angle, intracranial, single-isocenter, SRS treatments with multiple targets on the Varian Edge radiosurgery system. Adv Radiat Oncol 2017;2:494-502.
19. Xu H, Song K, Chetty I, Wen N, Kim J. SU-E-J-13: Six Degree of Freedom Image Fusion Accuracy for Cranial Target Localization On the Varian Edge Stereotactic Radiosurgery System: Comparison Between 2D/3D and KV CBCT Image Registration. Med Phys 2015;42:3266-66.
20. Al-Hallaq HA, Cerviño L, Gutierrez AN, Havnen-Smith A, Higgins SA, Kügele M, Padilla L, Pawlicki T, Remmes N, Smith K, Tang X, Tomé WA. AAPM task group report 302: Surface-guided radiotherapy. Med Phys 2022;49:e82-e112.
21. Hoisak JDP, Pawlicki T. The Role of Optical Surface Imaging Systems in Radiation Therapy. Semin Radiat Oncol 2018;28:185-93.
22. Walter F, Freislederer P, Belka C, Heinz C, Söhn M, Roeder F. Evaluation of daily patient positioning for radiotherapy with a commercial 3D surface-imaging system (Catalyst™). Radiat Oncol 2016;11:154.
23. Lai J, Liu J, Zhao J, Li A, Liu S, Deng Z, Tan Q, Wang H, Jia Y, Lei K, Zhou L. Effective method to reduce the normal brain dose in single-isocenter hypofractionated stereotactic radiotherapy for multiple brain metastases. Strahlenther Onkol 2021;197:592-600.
24. Lai J, Liu S, Liu J, Jia Y, Lei K, Li A, Deng Z, Li B, Wang H, Zhou L. Using a fixed-jaw technique to achieve superior delivery accuracy and plan quality in single-isocenter multiple-target stereotactic radiosurgery for brain metastases. Journal of Radiation Research and Applied Sciences 2022;15:76-83.
25. Klein EE, Hanley J, Bayouth J, Yin FF, Simon W, Dresser S, Serago C, Aguirre F, Ma L, Arjomandy B, Liu C, Sandin C, Holmes T, American Association of Physicists in Medicine. Task Group 142 report: quality assurance of medical accelerators. Med Phys 2009;36:4197-212.
26. Bland JM, Altman DG. Statistical methods for assessing agreement between two methods of clinical measurement. Lancet 1986;1:307-10.
27. Roper J, Chanyavanich V, Betzel G, Switchenko J, Dhabaan A. Single-Isocenter Multiple-Target Stereotactic Radiosurgery: Risk of Compromised Coverage. Int J Radiat Oncol Biol Phys 2015;93:540-6.
28. Tsui SSW, Wu VWC, Cheung JSC. Comparison of dosimetric impact of intra-fractional setup discrepancy between multiple- and single-isocenter approaches in linac-based stereotactic radiotherapy of multiple brain metastases. J Appl Clin Med Phys 2022;23:e13484.
29. Tarnavski N, Engelholm SA, Af Rosenschold PM. Fast intra-fractional image-guidance with 6D positioning correction reduces delivery uncertainty for stereotactic radiosurgery and radiotherapy. J Radiosurg SBRT 2016;4:15-20.
30. Li J, Shi W, Andrews D, Werner-Wasik M, Lu B, Yu Y, Dicker A, Liu H. Comparison of Online 6 Degree-of-Freedom Image Registration of Varian TrueBeam Cone-Beam CT and BrainLab ExacTrac X-Ray for Intracranial Radiosurgery. Technol Cancer Res Treat 2017;16:339-43.
31. Murphy MJ. The importance of computed tomography slice thickness in radiographic patient positioning for radiosurgery. Med Phys 1999;26:171-5.
32. Hoogeman MS, Nuyttens JJ, Levendag PC, Heijmen BJ. Time dependence of intrafraction patient motion assessed by repeat stereoscopic imaging. Int J Radiat Oncol Biol Phys 2008;70:609-18.
33. Chang J, Yenice KM, Narayana A, Gutin PH. Accuracy and feasibility of cone-beam computed tomography for stereotactic radiosurgery setup. Med Phys 2007;34:2077-84.
34. Corradetti MN, Mitra N, Bonner Millar LP, Byun J, Wan F, Apisarnthanarax S, Christodouleas J, Anderson N, Simone CB 2nd, Teo BK, Rengan R. A moving target: Image guidance for stereotactic body radiation therapy for early-stage non-small cell lung cancer. Pract Radiat Oncol 2013;3:307-15.
35. Gui LG, Shi M, Li J. Cone beam computed tomography and image registration based on target area for stereotactic body radiation therapy of lung cancer. Journal of Radiation

Research and Applied Sciences 2021;14:404-11.
36. Yoshidome S, Arimura H, Terashima K, Hirakawa M, Hirose TA, Fukunaga J, Nakamura Y, Honda H. Automated and robust estimation framework for lung tumor location in kilovolt cone-beam computed tomography images for target-based patient positioning in lung stereotactic body radiotherapy. Medical Imaging and Information Sciences 2018;35:48-54.
37. Guckenberger M, Baier K, Guenther I, Richter A, Wilbert J, Sauer O, Vordermark D, Flentje M. Reliability of the bony anatomy in image-guided stereotactic radiotherapy of brain metastases. Int J Radiat Oncol Biol Phys 2007;69:294-301.
38. Xu H, Brown S, Chetty IJ, Wen N. A Systematic Analysis of Errors in Target Localization and Treatment Delivery for Stereotactic Radiosurgery Using 2D/3D Image Registration. Technol Cancer Res Treat 2017;16:321-31.
39. Prentou G, Pappas EP, Logothetis A, Koutsouveli E, Pantelis E, Papagiannis P, Karaiskos P. Dosimetric impact of rotational errors on the quality of VMAT-SRS for multiple brain metastases: Comparison between single- and two-isocenter treatment planning techniques. J Appl Clin Med Phys 2020;21:32-44.
40. Gevaert T, Verellen D, Engels B, Depuydt T, Heuninckx K, Tournel K, Duchateau M, Reynders T, De Ridder M. Clinical evaluation of a robotic 6-degree of freedom treatment couch for frameless radiosurgery. Int J Radiat Oncol Biol Phys 2012;83:467-74.
41. Babic S, Lee Y, Ruschin M, Lochray F, Lightstone A, Atenafu E, Phan N, Mainprize T, Tsao M, Soliman H, Sahgal A. To frame or not to frame? Cone-beam CT-based analysis of head immobilization devices specific to linac-based stereotactic radiosurgery and radiotherapy. J Appl Clin Med Phys 2018;19:111-20.

Cite this article as: Lai J, Liu S, Liu J, Fu M, Jiang M, Li A, Li B, Li X, Cheng X, Zhou L. Going from 3D/3D to 2D/3D registration for noncoplanar setup verification in intracranial single-isocenter multiple-target hypofractionated stereotactic radiotherapy: comparison between kilo-voltage/mega-voltage image pairs and noncoplanar cone-beam computed tomography. Quant Imaging Med Surg 2023;13(12):8094-8106. doi: 10.21037/qims-23-463

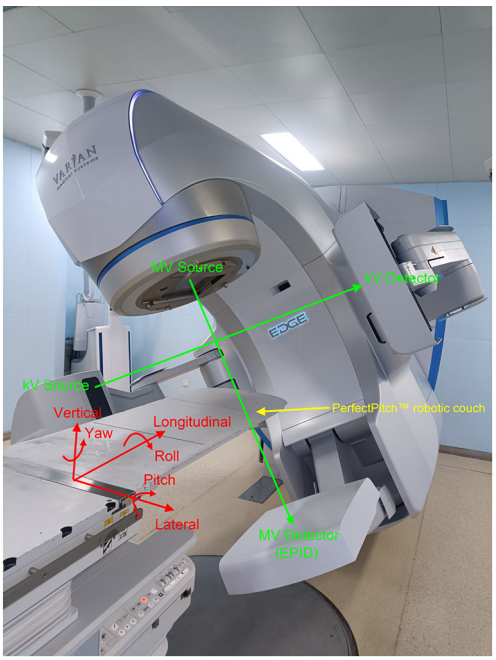

Figure S1 Picture of the Edge™ LINAC, which is equipped with kV and MV imagers and a 6DOF PerfectPitch™ couch. The coordinate system used in this study is shown. All arrows point in the positive directions in 6DOF. MV, mega-voltage image; kV, kilo-voltage; EPID, electronic portal imaging device; LINAC, linear accelerator; 6DOF, six degrees of freedom.

Table S1 The available cone-beam CT scanning range and gantry angle for kV/MV image pairs acquisition corresponding to couch angle

Couch angle (°)	CBCT scanning range (°)	Arc length (°)	Gantry angle for kV/MV image pairs acquisition (°)
0	180–340	200	181
350	180–340	200	180
340	180–340	200	180
330	180–340	200	180
320	131–306	185	0
315	132–305	187	0
10	180–340	200	181
20	181–21	200	181
30	181–21	200	181
40	181–337	156	181
45	181–336	155	181

CT, computed tomography; kV/MV, kilo-voltage/mega-voltage image; CBCT, cone-beam computed tomography.

https://dx.doi.org/10.21037/qims-23-463